Image segmentation using random-walks on the histogram

Jean-Philippe Morin[a], Christian Desrosiers[a] and Luc Duong[a]

[a]Ecole de technologie superieure, 1100 Notre-Dame St. W., Montreal, Canada

ABSTRACT

This document presents a novel method for the problem of image segmentation, based on random-walks. This method shares similarities with the Mean-shift algorithm, as it finds the modes of the intensity histogram of images. However, unlike Mean-shift, our proposed method is stochastic and also provides class membership probabilities. Also, unlike other random-walk based methods, our approach does not require any form of user interaction, and can scale to very large images. To illustrate the usefulness, efficiency and scalability of our method, we test it on the task of segmenting anatomical structures present in cardiac CT and brain MRI images.

Keywords: Image segmentation, random-walk, intensity histogram, coronary CT, brain MRI

1. INTRODUCTION

Automatic image segmentation is an unsupervised learning problem where one must cluster the pixels of an image, often encoded as a single intensity value, into regions representing structures or objects in the image. This well-known problem has several key applications, including image compression and recoloring, as well as automated classification and tracking of objects and structures in images. In many cases, the pixels of given regions in images share similar values, either color or intensity, because they encode some intrinsic properties of these regions. For example, CT images are obtained by placing the scanned object or patient between an X-ray beam and a detector. The intensity value of pixels is mostly determined by the physical properties of material (e.g, fat, muscle or tissue) and its thickness. For such images, a good segmentation can be obtained by only considering the distribution of pixels values, which corresponds to the image histogram. An example of a CT image, showing the aorta and coronary arteries, and the intensity histogram of this image, are shown in Figure 1.

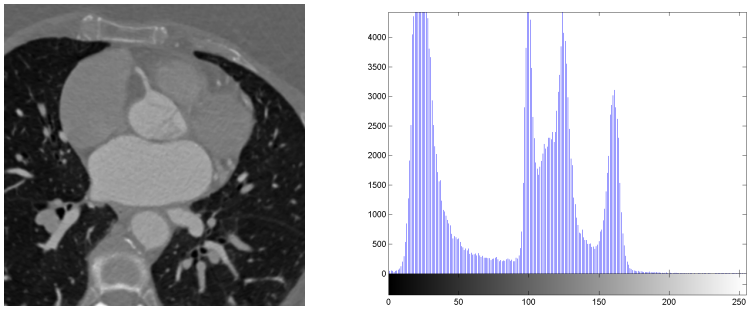

Figure 1. Cardiac CT slice and its histogram of intensity values.

In this paper, we present a novel image segmentation method that uses random-walks to find the peaks (modes) within the intensity histogram of images, and cluster pixels around these peaks. This method is similar to two popular segmentation approaches, the Mean-shift (see Comaniciu et al.[1]) and Random-walker (Grady[2]) algorithms. Thus, like Mean-shift, our approach works exclusively on the intensity histogram, which allows it to scale to very large images. However, similar to the Random-walker algorithm, our method uses a probabilistic formulation which allows us to find class membership probabilities for each pixel, instead of a simple class value. In comparison to these segmentation algorithms, our proposed method has several advantages:

Further author information:
Christian Desrosiers: E-mail: christian.desrosiers@etsmtl.ca, Telephone: 1 514 396 8531
Luc Duong: E-mail: luc.duong@etsmtl.ca, Telephone: 1 514 396 8827

1. In contrast to Random-walker, which requires users to manually label foreground and background pixels in the image, our approach is fully automatic and requires no such user interaction. This is a significant advantage in cases where a great number of images need to be segmented, and the user does not have enough time for such a task.

2. As mentioned above, our method returns class membership probabilities, instead of simple class values. This additional information could be valuable to identify overlapping or ill-defined structures in the image, or could provide more significant inputs to a classification method.

3. Finally, our method is more efficient than both the Mean-shift and Random-walker algorithms. Thus, unlike Random-walker, its complexity is *linear* to the number of pixels, which allows it to scale to very large images. Also, as opposed to Mean-shift, our method is not iterative and can be computed very efficiently by inverting a tridiagonal matrix, the complexity of which is *quadratic* to the number of intensity values.

The rest of this paper is structured as follows. The next section presents a short review of the relevant literature on image segmentation. We then present the details of our segmentation approach and evaluate its usefulness, efficiency and scalability on the task of segmenting cardiac CT and brain MRI images. We end the paper with a brief summary of our contributions and results.

2. REVIEW OF LITERATURE

Numerous approaches have been proposed for the segmentation of medical images. Such approaches are normally grouped into two main categories: semi-automatic and (fully) automatic methods. Semi-automatic methods, such as the Random-walker algorithm proposed by Grady[2] and other methods based on graph-cuts (e.g., see Funka-Lea et al.[3]), require the user to provide seed points within the regions to segment. As mentioned above, while these methods allow a finer control of the segmentation process and results, they are not practical when a large batch of images needs to be segmented. Automatic methods, on the other hand, do not require any manual interaction. Several types of automated methods have been proposed over the years, including methods based on clustering (e.g., Sikka et al.[4]), level-sets (e.g., Liu et al.[5]) and active contours (e.g., Gao et al.[6]). Recently, many researches have focused on the development of atlas-based methods, which use one or several pre-labeled templates to segment a new image. Among these approaches are methods based on least square support vector machines (e.g., Kasiri et al.[7]), intensity classification (e.g., Sdika et al.[8]), Markov random fields (e.g., Bauer et al.[9]), decision fusion (e.g., Rohlfing et al.[10]) and graph cuts (e.g., Lotjonen et al.[11]). For a more extensive survey of the literature on atlas-based segmentation, the reader can refer to Cabezas et al.[12]

Because of their greater efficiency, many histogram-based methods have also been proposed for the task of segmenting medical images. For instance, a simple method based on Otsu's thresholding technique[13] was proposed by Shan et al.[14] to segment brain MR volumes. Moreover, Seo et al.[15] proposes a method to tail-threshold the histogram of intensities and uses this method to segment images of liver tissues. Also, Nakib et al.[16] uses 2D histograms (intensities and their spatial correspondences) to segment brain images. Finally, Dou et al.[17] segment brain MRI images using a fuzzy-clustering algorithm on the histogram. While the method proposed in this paper also uses the histogram to provide a fast automatic segmentation, it has the additional benefits of requiring little parameter tuning and of providing class membership probabilities.

3. STOCHASTIC SEGMENTATION USING THE HISTOGRAM

This section describes our proposed segmentation method and provides some information on its complexity and possible extensions.

3.1 Random-walk formulation

To find the peaks in the histogram, we consider it as a landscape on which is moving a random walker. For each intensity level i in the histogram, we assign i to the level j that has the greatest chance of being visited by a walker starting at i. Figure 2 shows the landscape resulting from the histogram values $h(i)$. This stochastic process can be represented using a graph where each node i corresponds to an intensity value, and the transition

probability $w_{i,j}$ from i to a neighbor node $j \in \{i-1,\, i,\, i+1\}$ is proportional to the difference of corresponding intensities in the histogram:

$$w_{i,j} \;=\; \phi\left(\frac{h(j)-h(i)}{N_{\text{pix}} \cdot N_{\text{int}}}\right), \tag{1}$$

where N_{pix} and N_{int} correspond to the number of pixels and intensity values used to compute the histogram. Moreover, ϕ is a function which maps the differences to the interval $[0,1]$, for instance, the sigmoid function:

$$\phi(x) \;=\; \frac{1}{1+\exp\{-(cx+d)\}}. \tag{2}$$

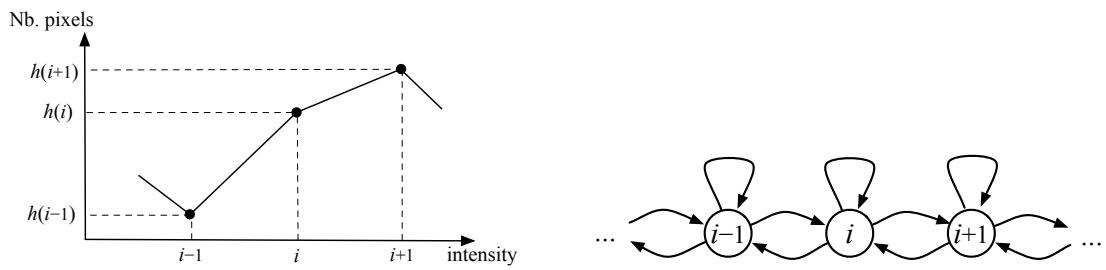

(a) (b)

Figure 2. (a) Landscape function defined by the intensity histogram, and (b) graph representing the random-walk process on this landscape.

By normalizing the transition probabilities, we obtain the transition matrix W such that:

$$W_{i,j} \;=\; \begin{cases} \frac{w_{i,j}}{w_{i,i-1} \,+\, w_{i,i} \,+\, w_{i,i+1}}, & \text{if } |i-j| \leq 1, \\ 0, & \text{otherwise.} \end{cases} \tag{3}$$

Suppose that the random-walk started at a node i of the graph and that, at a certain time t, the walker is at node j. The transition process can be described using a single parameter $\alpha \in [0,1]$:

1. With probability $(1-\alpha)$, the walker chooses a node $j' \in \{j-1,\, j,\, j+1\}$ with probability $W_{j,j'}$, and moves to this node;
2. Otherwise, with probability α, the walker returns to the starting node i.

Thus, α controls the locality of the walk (how far from the initial node the walker can stray). If $\alpha = 1$, then the walk will stay at the initial node, and the segmented image will be identical to the original one. Reversely, if $\alpha = 0$, then the walk will be unrestricted and will tend to visit higher peaks more often. Hence, the segmented image will be such that all pixels are mapped to the most frequent intensity in the histogram.

The probability of a random-walk, starting at node i, to be at node j at a given time t is therefore:

$$\pi_{i,j}(t+1) \;=\; (1-\alpha)\Big[W_{j-1,j}\,\pi_{i,j-1}(t) \;+\; W_{j+1,j}\,\pi_{i,j+1}(t) \;+\; W_{j,j}\,\pi_{i,j}(t)\Big] \;+\; \alpha\,\delta(i=j), \tag{4}$$

where $\delta(i=j)=1$ if $i=j$, otherwise 0. Considering every initial node i and every visited node j, this relation can be expressed in matrix form as:

$$P_{t+1} \;=\; (1-\alpha)P_t\,W \;+\; \alpha\,I, \tag{5}$$

where the i-th line of P_t gives the walk probabilities at time t of a random-walk starting at node i. Since there is a non-zero probability of reaching any node from any other node, we can show there exists a *stable state* $P_\infty = P$ such that:

$$P \;=\; \alpha\,[I-(1-\alpha)W]^{-1}. \tag{6}$$

The class of an intensity level i then corresponds to the most probable node j in P, for a random-walk starting at i:

$$C(i) \;=\; \arg\max_j \{P_{i,j}\}. \tag{7}$$

3.2 Complexity and other considerations

Because matrix $I - (1-\alpha)W$ is tridiagonal, its inverse can be computed in $O(N^2)$ steps, where the matrix size N corresponds to the number of intensity levels in the image (see El-Mikkawy et al.[18] for a proof). Moreover, the computation of P can be interpreted as the diffusion of probability values in the transition matrix W:

$$P = \alpha \sum_{k=0}^{\infty} (1-\alpha)^k W^k. \tag{8}$$

Thus, the random-walk formulation of our method is consistent with the initial hypothesis that pixel intensities are generated by applying small perturbations (noise) to the representative intensity of the corresponding class.

While this method has three distinct parameters (α, c and d), parameters c and d depend mostly on the number of pixels and intensity values in the image, and require almost no image-specific tuning. Moreover, because this approach is very efficient, even for very large images, it is possible to compute the segmentation for various values of α and select a proper value based on the number of obtained classes. Finally, although the proposed method was formulated only for intensity (gray) level images, the same idea could be used to segment color images. Thus, we could build a 3D histogram, having a dimension for each of the RGB or HSV components and, as explained above, translate this histogram into a graph. While, the resulting transition matrix would not be tridiagonal, this matrix would be very sparse and, therefore, easily invertible.

4. EXPERIMENTAL RESULTS

We evaluated the efficiency and scalability of our method on the task of segmenting cardiac CT and brain MRI images. We compared our method with the Mean-shift algorithm, since both approaches work by finding modes in the histogram, and do not require any form of user interaction. For Mean-shift, we used the open source Matlab package implemented by Y. Keselman,[19] and kept the default parameter setting: window width $w = 20$, size of color group $g = 200$, and minimal region size $r = 20$. We found this setting to give reasonably good results for most tested images. Our segmentation algorithm was also implemented in Matlab. All tests were carried out on a 2.30 Ghz i7 64 bit Intel CPU computer, with 8 Go of RAM.

4.1 Cardiac CT segmentation

Figure 3 shows the segmentation of the CT image of Figure 1, obtained by our method using various values of α, and by the Mean-shift algorithm. We can see that our method gives results similar to Mean-shift for $\alpha = 7.0 \times 10^{-6}$, and that a coarser segmentation can be obtained by decreasing α. Figure 3 compares the segmentation of Mean-shift with the one obtained by our method, on three other cardiac CT images. Once again, the results of Mean-shift and our method are similar in quality.

While our random-walk based method achieved segmentation results similar to those obtained with Mean-shift, we found it to be more efficient. As shown in Table 1, our method is consistently faster than Mean-shift, and scales linearly to the number of image pixels.

Table 1. Average runtimes (in seconds) obtained by our random-walk based method and the Mean-shift algorithm over 10 benchmark images of increasing size (pixels).

Image size	Random-walk	Mean-shift
256×256	0.027	1.193
512×512	0.035	4.427
1024×1024	0.061	17.572
2048×2048	0.161	73.213
4096×4046	0.569	293.262

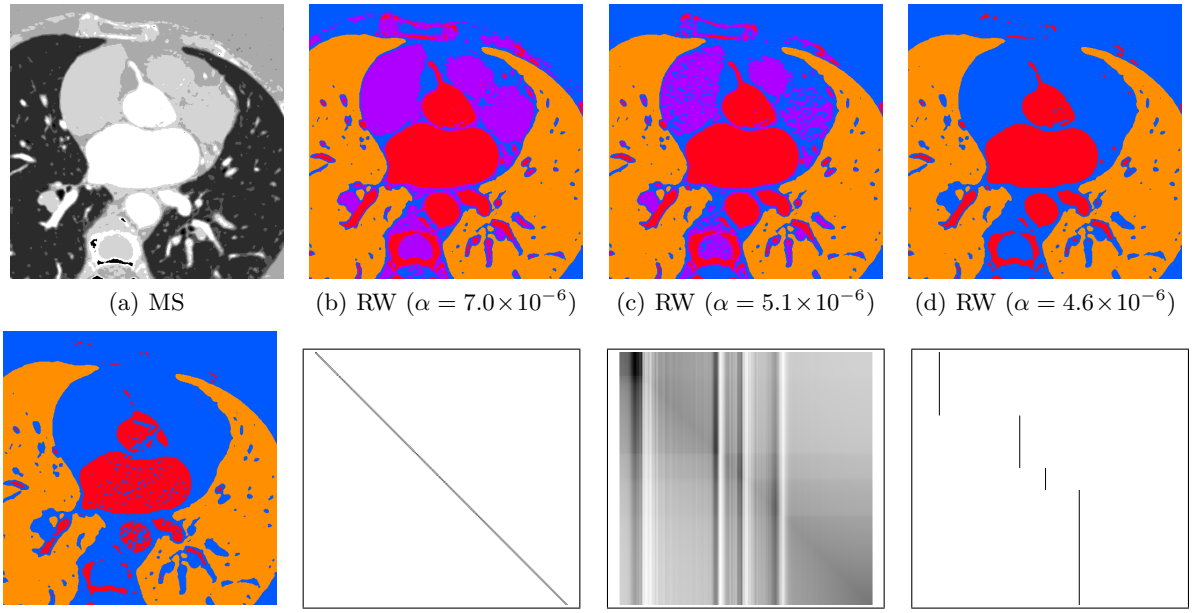

(a) MS (b) RW ($\alpha = 7.0\times10^{-6}$) (c) RW ($\alpha = 5.1\times10^{-6}$) (d) RW ($\alpha = 4.6\times10^{-6}$)

(e) RW ($\alpha = 3.2\times10^{-6}$) (f) Matrix W (g) Matrix P (h) Matrix C

Figure 3. Segmentation results obtained with (a) the Mean-shift (MS) algorithm, and (b)-(e) our random-walk (RW) based method using $c = 250000$, $d = 0$ and decreasing values of α. Mean-shift parameters used are: window width $w = 20$, size of color group $g = 200$, and minimal region size $r = 20$. Subfigures (f)-(h) show the tridiagonal transition matrix W, the random-walk probability matrix P, and the line-wise maximum matrix C, for the parameter setting of (b). Darker pixels correspond to higher probability values.

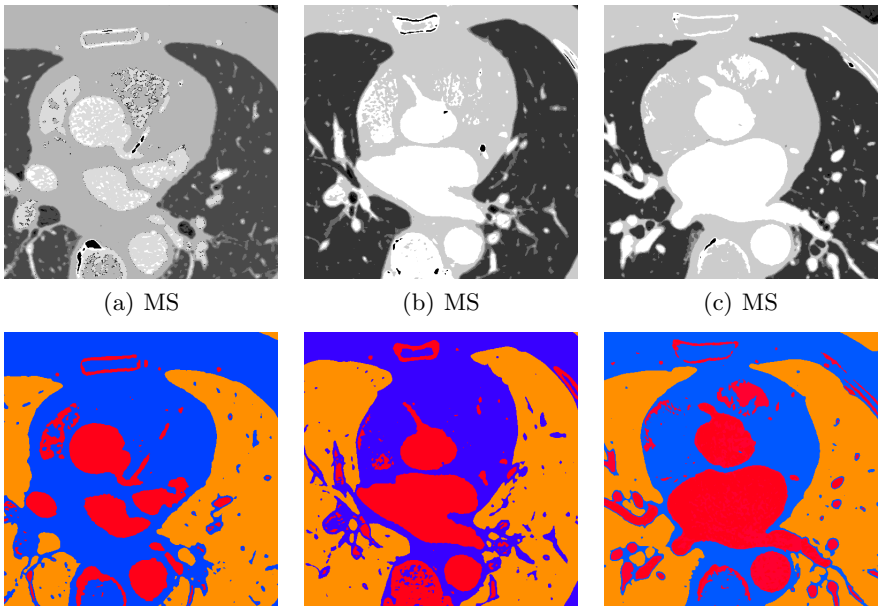

(a) MS (b) MS (c) MS

(d) RW ($\alpha = 5.8\times10^{-6}$) (e) RW ($\alpha = 1.9\times10^{-6}$) (f) RW ($\alpha = 4.4\times10^{-6}$)

Figure 4. (*top-row*) Segmentation results obtained by Mean-shift (MS), and (*bottom-row*) results obtained by our method (RW) for the same images, using $c = 250000$, $d = 0$ and specified values of α. Mean-shift parameters used are: window width $w = 20$, size of color group $g = 200$, and minimal region size $r = 20$.

4.2 Brain MRI segmentation

We also tested our method on the task of segmenting brain MRI data, obtained from the Internet Brain Segmentation Repository (IBSR) database.[20] This dataset contains several volumes (brains) composed of images

representing 3.0mm thick slices. Following similar works in the literature, the objective is to segment the volumes into four distinct classes: whiter matter (WM), gray matter (GM), cerebro-spinal fluid (CSF), and background (BG). To evaluate the quality of the segmentations, we use the Dice index. Let C_{GT} and C_{RW} denote, respectively, the set of pixels corresponding to a given class (the *ground-truth* of the class) and the pixels mapped to that class by our method. The Dice index is computed as

$$\mathrm{Dice}(C_{\mathrm{GT}}, C_{\mathrm{RW}}) \;=\; \frac{2|C_{\mathrm{GT}} \cap C_{\mathrm{RW}}|}{|C_{\mathrm{GT}}| + |C_{\mathrm{RW}}|}. \tag{9}$$

To map the classes obtained by our method to those of the ground-truth, we use the following rule: a class C_{RW} is mapped to the class C_{GT} with which it has the greatest intersection $|C_{\mathrm{RW}} \cap C_{\mathrm{GT}}|$.

Figure 5 gives the Dice index and number of classes obtained on three different volumes, for increasing values of α. For the computation of the Dice index, we set parameter c to 500000. While good segmentation results were obtained for the WM and GM classes (Dice index ranging from 0.58 to 0.92), the results obtained for the CSF class are not as satisfactory. However, upon examination, it was discovered that regions corresponding to CSF were indeed found by our method, but these regions were mapped to the GM class in the post-processing step, due to the fact that pixels located in a thin layer surrounding the brain have similar intensity values. Moreover, although many classes can be obtained for higher values of α, we noticed that most of these classes contain only a few pixels. Examples of segmentation results are shown in Figure 6. We can see that the regions obtained by our method are visually more similar to the ground-truth than those obtained by Mean-shift.

5. CONCLUSION

This study proposed a new segmentation method based on the random-walk traversal of image histograms. This simple method does not require any form of user interaction and is more efficient than other random-walk approaches such as Random-walker. Moreover, computational experiments on the task of segmenting CT and MRI images have shown our method to give results equivalent to those obtained by the well-known Mean-shift algorithm, faster than this algorithm. Finally, our method can be used as a preprocessing step for a finer interactive segmentation algorithm. **The work has not been submitted elsewhere**.

REFERENCES

[1] Comaniciu, D. and Meer, P., "Robust analysis of feature spaces: color image segmentation," in [*Proc. of the IEEE Conference on Computer Vision and Pattern Recognition*], 750–755 (June 1997).

[2] Grady, L., "Random walks for image segmentation," *IEEE Transactions on Pattern Analysis Machine Intelligence* **28**, 1768–1783 (November 2006).

[3] Funka-Lea, G., Boykov, Y., Florin, C., Jolly, M.-P., Moreau-Gobard, R., Ramaraj, R., and Rinck, D., "Automatic heart isolation for ct coronary visualization using graph-cuts," in [*Biomedical Imaging: Nano to Macro, 2006. 3rd IEEE International Symposium on*], 614 –617 (april 2006).

[4] Sikka, K., Sinha, N., Singh, P. K., and Mishra, A. K., "A fully automated algorithm under modified FCM framework for improved brain MR image segmentation," *Magnetic Resonance Imaging* **27**(7), 994 – 1004 (2009).

[5] Liu, J., Chelberg, D., Smith, C., and Chebrolu, H., "Distribution-based level set segmentation for brain MR images," in [*BMVC07*], (2007).

[6] Gao, S. and Bui, T., "Image segmentation and selective smoothing by using Mumford-Shah model," *Image Processing, IEEE Transactions on* **14**, 1537 –1549 (oct. 2005).

[7] Kasiri, K., Kazemi, K., Dehghani, M., and Helfroush, M., "Atlas-based segmentation of brain MR images using least square support vector machines," in [*Image Processing Theory Tools and Applications (IPTA)*], 306 –310 (2010).

[8] Sdika, M., "Combining atlas based segmentation and intensity classification with nearest neighbor transform and accuracy weighted vote," *Medical Image Analysis* **14**(2), 219 – 226 (2010).

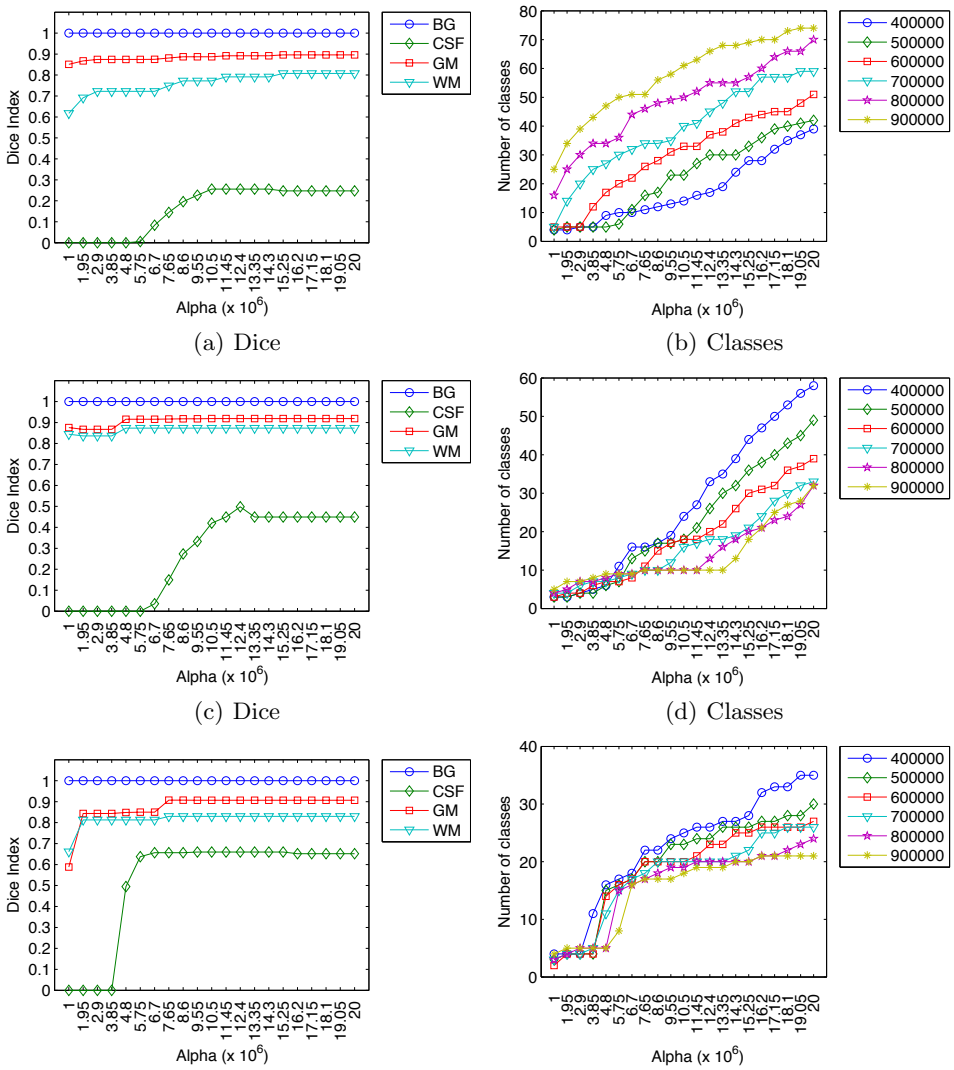

(a) Dice (b) Classes

(c) Dice (d) Classes

(e) Dice (f) Classes

Figure 5. Segmentation results for the IBSR brain dataset. Each row shows for a different patient, and using increasing values of α: (*on the left*) the Dice index for each region type, Cerebro-spinal fluid (CSF), gray matter (GM), White matter (WM) and Background (BG), as well as (*on the right*) the number of classes obtained by our method. For the Dice index, we used $c = 500000$. For both the Dice index and the number of classes, we used $d = 0$. The histograms were computed on the volumes (all slices at once).

[9] Bauer, S., Nolte, L., and Reyes, M., "Segmentation of brain tumor images based on atlas-registration combined with a markov-random-field lesion growth model," in [*IEEE Int. Symposium on Biomedical Imaging*], 2018–2021 (2011).

[10] Rohlfing, T. and Jr., C. M., "Multi-classifier framework for atlas-based image segmentation," *Pattern Recognition Letters* **26**(13), 2070 – 2079 (2005).

[11] Lotjonen, J., Wolz, R., Koikkalainen, J., Thurfjell, L., Waldemar, G., Soininen, H., and Rueckert, D., "Fast and robust multi-atlas segmentation of brain magnetic resonance images," *NeuroImage* **49**(3), 2352 – 2365 (2010).

[12] Cabezas, M., Oliver, A., Llado, X., Freixenet, J., and Bach Cuadra, M., "A review of atlas-based segmentation for magnetic resonance brain images," *Computer methods and programs in biomedicine* **104**, 158–177 (2011).

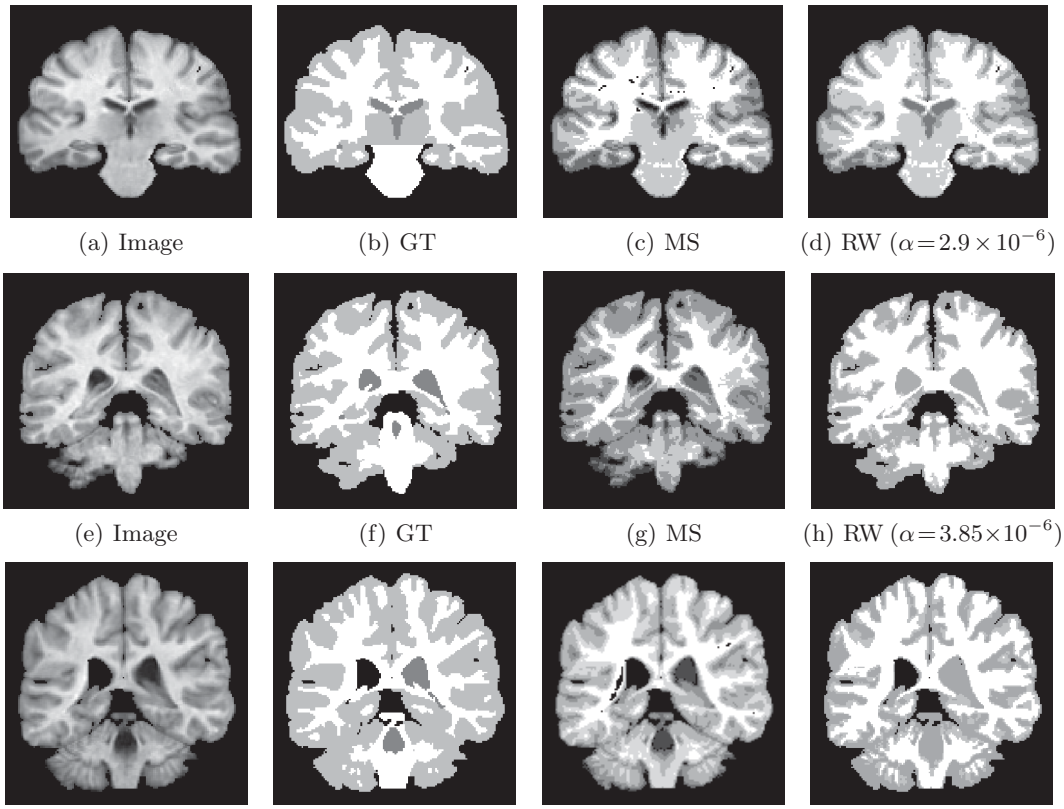

(a) Image (b) GT (c) MS (d) RW ($\alpha = 2.9 \times 10^{-6}$)

(e) Image (f) GT (g) MS (h) RW ($\alpha = 3.85 \times 10^{-6}$)

(i) Image (j) GT (k) MS (l) RW ($\alpha = 2.9 \times 10^{-6}$)

Figure 6. Examples of segmentation results obtained for the IBSR brain dataset. Each of the three rows shows the segmentation obtained for a different patient (the same ones as in Figure 5). From left to right, each row contains the original image, ground-truth (GT), and segmentation results obtained by the Mean-shift algorithm (MS) and our random-walk (RW) approach on the 24th brain slice of each patient. For Mean-shift, we used the default parameters: window width $w = 20$, size of color group $g = 200$, and minimal region size $r = 20$. For our method, we used $c = 500000$, $d = 0$ and the specified α values. For both methods, the histograms were computed on the volumes (all slices at once).

[13] Otsu, N., "A threshold selection method from gray level histograms," *IEEE Trans. Systems, Man and Cybernetics* **9**, 62–66 (Mar. 1979).

[14] Shan, Z., Yue, G., and Liu, J., "Automated histogram-based brain segmentation in T1-weighted three-dimensional magnetic resonance head images," *NeuroImage* **17**(3), 1587 – 1598 (2002).

[15] Seo, K.-S., "Improved fully automatic liver segmentation using histogram tail threshold algorithms," in [*Computational Science ICCS 2005*], Sunderam, V., van Albada, G., Sloot, P., and Dongarra, J., eds., *Lecture Notes in Computer Science* **3516**, 61–150, Springer Berlin / Heidelberg (2005).

[16] Nakib, A., Roman, S., Oulhadj, H., and Siarry, P., "Fast brain MRI segmentation based on two-dimensional survival exponential entropy and particle swarm optimization.," *Proc. of IEEE Engineering in Medicine and Biology Society* **1**(2), 5563–5566 (2007).

[17] Dou, W., Ren, Y., Chen, Y., Ruan, S., Bloyet, D., and Constans, J.-M., "Histogram-based generation method of membership function for extracting features of brain tissues on MRI images," in [*Fuzzy Systems and Knowledge Discovery*], **3613**, 476–476, Springer Berlin / Heidelberg (2005).

[18] El-Mikkawy, M. and Karawia, A., "Inversion of general tridiagonal matrices," *Applied Mathematics Letters* **19**, 712–720 (August 2006).

[19] Keselman, Y., "Mean-shift image segmenter package for Matlab." `http://yashma.org/yakovkeselman/Software/ms_segmenter.html`.

[20] "Internet brain segmentation repository (IBSR)." http://www.cma.mgh.harvard.edu/ibsr/.